A DIRECT MEASUREMENT OF INTENSITIES
IN
A FRESNEL DIFFRACTION PATTERN

THESIS FOR THE DEGREE OF M. S.

CYRIL ELWIN MCCLELLAN

1938

A DIRECT MEASUREMENT OF INTENSITIES IN A FRESNEL DIFFRACTION PATTERN

Cyril Elwin McClellan

THESIS

Submitted in partial fulfillment of the requirements for the Degree of Master of Science

Michigan State College

1938

CONTENTS

	Page
INTRODUCTION	1
APPARATUS	2
CALIBRATION OF AMPLIFIER	11
MEASUREMENT OF DIFFRACTION PATTERNS	16
COMPARISON WITH THEORETICAL VALUES	19
DISCUSSION OF ERRORS	27
CONCLUSIONS	31
ACKNOWLEDGMENT	32
BIBLIOGRAPHY	33

A DIRECT MEASUREMENT OF INTENSITIES IN A FRESNEL DIFFRACTION PATTERN

INTRODUCTION

In the years of 1815-16 Fresnel propounded to the French Academy of Sciences his theory of diffraction, supported by such conclusive experimental evidence that the intervening years have resulted in mere mathematical elaboration of his fundamental concepts and but little quantitative investigation of his experimental evidence.[1] Because of the non-existence of apparatus capable of measuring the distribution of the energy in the patterns which he studied, Fresnel was limited to a visual observation of the location of the maxima and minima. The only qualitative measurements to which any reference has been found were reported by Lyman of Harvard University in 1929.[2] His method consisted of photographing a straight edge diffraction pattern and measuring it with a microphotometer. The exposure-density curve of the photographic plate was made at the same time and from it the microphotometer trace was corrected to give the actual distribution of the light intensity. He records only the intensity ratios of succeeding maxima, which check the theoretical values within his estimated probable error of 4%.

In connection with the construction of apparatus for the measurement of very faint light, which was done in the Physics Department of the Michigan State College during the summer of 1937, it was thought worthwhile to attempt a direct measurement of the energy distribution throughout a diffraction pattern. For this purpose the diffraction pattern due to a single narrow slit was chosen. In the single slit pattern used the intensity of illumination at the first minimum is about 2×10^{-5} times the intensity of the first minimum of a straight edge pattern produced by the same optical system. A typical straight edge pattern is shown in Fig. 1.

Fig. 1. Photograph of a single narrow slit diffraction pattern.

APPARATUS

The pattern was produced by a single narrow slit, approximately 0.025 centimeters wide, and was measured at a distance of $204.0 \pm .5$ cms. from the slit. There is considerable possible error in the width of the slit given because, due to a multiplicity of arms and levers in its construction, there was an unknown amount of springing when it was clamped down on the sheet of celluloid which was used for a thickness gauge. A more accurate value was calculated from observed data.

The slit was fastened at one end of a light tight wooden box, two meters long, and finished a dull black inside. At the other

end was mounted the apparatus for measuring the light intensity. An optical diagram is shown in Fig. 2. Unfortunately there was no source of monochromatic light available of sufficient intensity to permit the measurements to be made and perforce a tungsten lamp was used. Corning filters G34Y and Didymium (now numbers 351 and 512 respectively) were used to isolate a portion of the continuous spectrum emitted by the tungsten. The lamp was a Westinghouse 100 watt projection lamp of the ribbon filament variety. The ribbon, 0.001 inches thick according to the manufacturers, was turned edgewise to the slit to approximate a point source, or in this case a line source and was 102.0 ± .4 cms. from the diffracting slit.

The light sensitive element of the apparatus was a Visitron type 53-AV vacuum photoelectric cell. This type of cell is in common commercial use and has well known characteristics. It consists of a cesium coated semi-circular plate 5/8 inch in diameter and 1 inch long. A small concentric wire when made positive with respect to the plate, collects the photoelectrons emitted by the cesium. Immediately in front of the cell was a slit, 2.5 by .08 cms., parallel to the diffracting slit. The position of the cell was such that the light coming through the slit always hit on the sensitive surface. A General Electric type FP-54 electrometer tube was coupled directly to the photoelectric cell and was used for thermionic amplification of the current flowing through the photoelectric cell. This tube was placed with the photoelectric cell in a copper box. The whole was mounted on a movable bed in such a fashion that the rotation of a screw would move the light gathering system across the pattern in a direction perpendicular to the optic axis and also

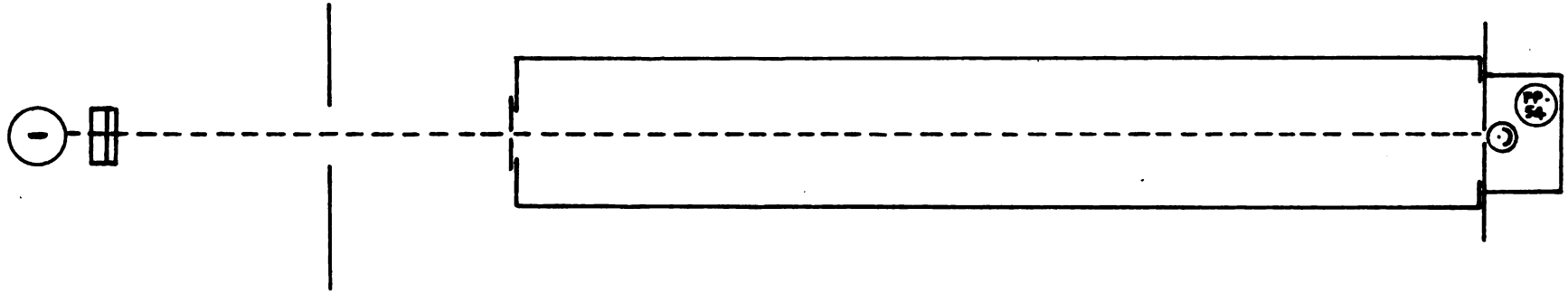

TOP VIEW OF OPTICAL SYSTEM

FIG. 2

to the fringes. The pitch of the screw was twenty threads per inch, which accounts for the apparent inconsistency of expressing this one measurement in inches at some places in this paper. However, the integer values which resulted from making one revolution of the screw at a time are very useful in reaching. Inside the copper box, in addition to the tube and the cell, were a bias battery, a calcium chloride drying tube, and an opaque shield to prevent light from the tube filament from reaching the cell. Connections from the movable box to a control box were made through a shielded flexible cable.

The type FP-54 tube is designed with special characteristics to facilitate the amplification of extremely small currents. It has a low filament operating temperature which contributes to high stability while its low plate potential gives high sensitivity to changes in the potential of the grid. The latter also prevents the formation of any gaseous ions within the tube. Two unique features of this tube are its space charge grid, located between the filament and the control grid, and the extremely high ohmic resistance between the grid and the other elements of the tube. The effect of the control grid on the space charge grid is the basis of a precision amplifying circuit. When the space charge grid is at a positive potential with respect to the filament, a decrease of the negative potential of the control grid causes a decrease in the current flowing in the space charge grid circuit and an increase in the current flowing through the plate circuit. (This is easily explained by a consideration of the electrostatic forces acting on electrons emitted from the filament). This behavior was applied

by DuBridge and Brown,[3] who, adapting a circuit developed by Soller,[4] have built the tube into a sort of a Wheatstone bridge circuit, the essentials of which are shown in Fig. 3.

In this circuit the plate and space charge grid of the tube are in opposite arms of a Wheatstone bridge. As mentioned above, a change in the grid bias changes the resistance of these two elements of the tube in opposite senses, thus unbalancing the bridge. Some idea of the sensitivity of this system may be obtained from the fact that a change of grid potential of one thousandth of a volt gave a galvanometer deflection of approximately one millimeter and corresponds to a change in grid current of 2×10^{-14} amperes. A grid voltage change, however, is not the only variable which will unbalance the bridge. Any variation in filament current will disturb the two branches and upset the balance. The imperfect regulation of all common sources of filament power led to the final adoption of a series parallel combination of 32 dry cells arranged to give 12 volts. Even this combination could not maintain its terminal voltage at the modest current drain of 70 milliamperes. The amount of this drop is shown in Fig. 4.

The bridge circuit is admirably adapted for compensating for this small voltage change and the resultant change in filament emission. Referring to Fig. 3, it will be readily seen that when there is no current flowing through the galvanometer

$$I_p R_p = I_s R_s \qquad (1)$$

where the subscripts refer to the plate series resistance and the space charge grid series resistance respectively. The effect of a change of filament current on the plate and space charge grid currents is shown in Table I and Fig. 5. Now if the galvanometer is to

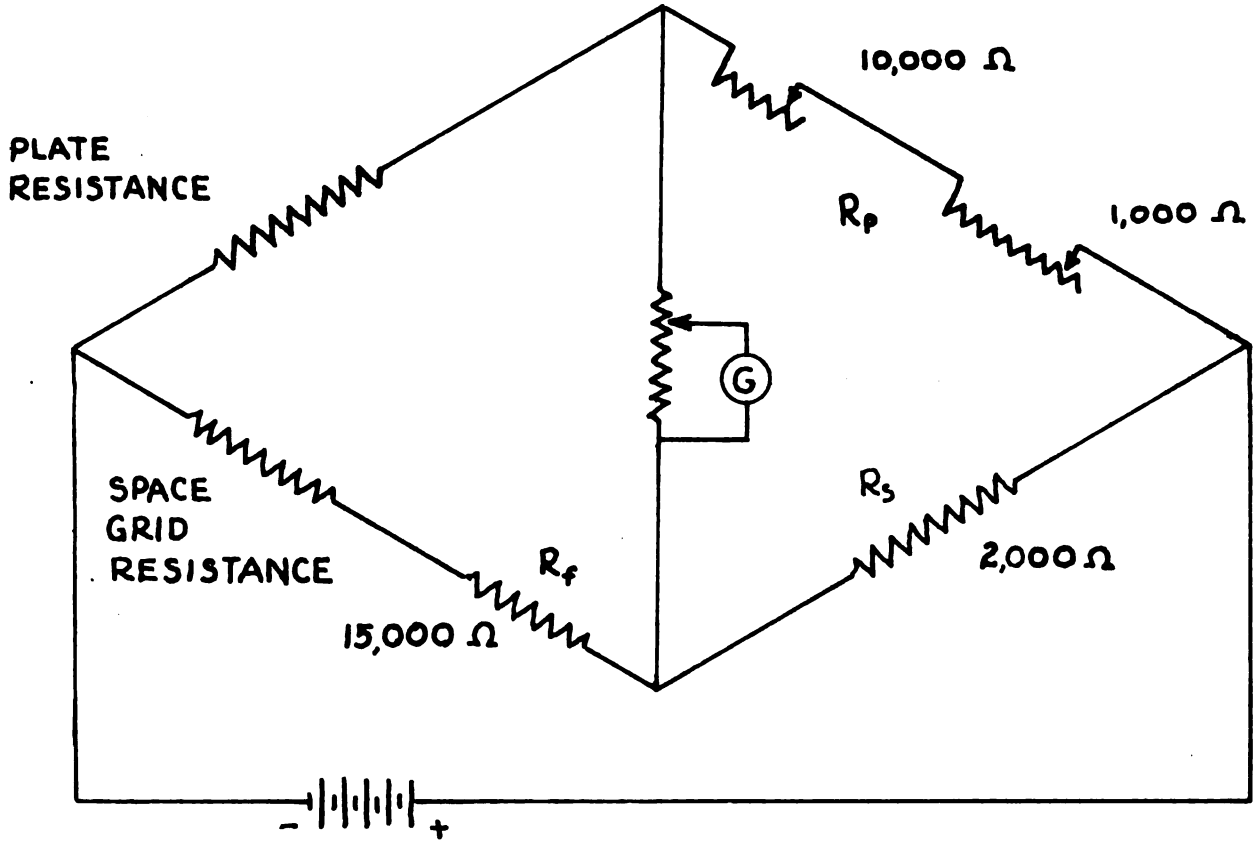

EFFECTIVE AMPLIFIER CIRCUIT

FIG. 3

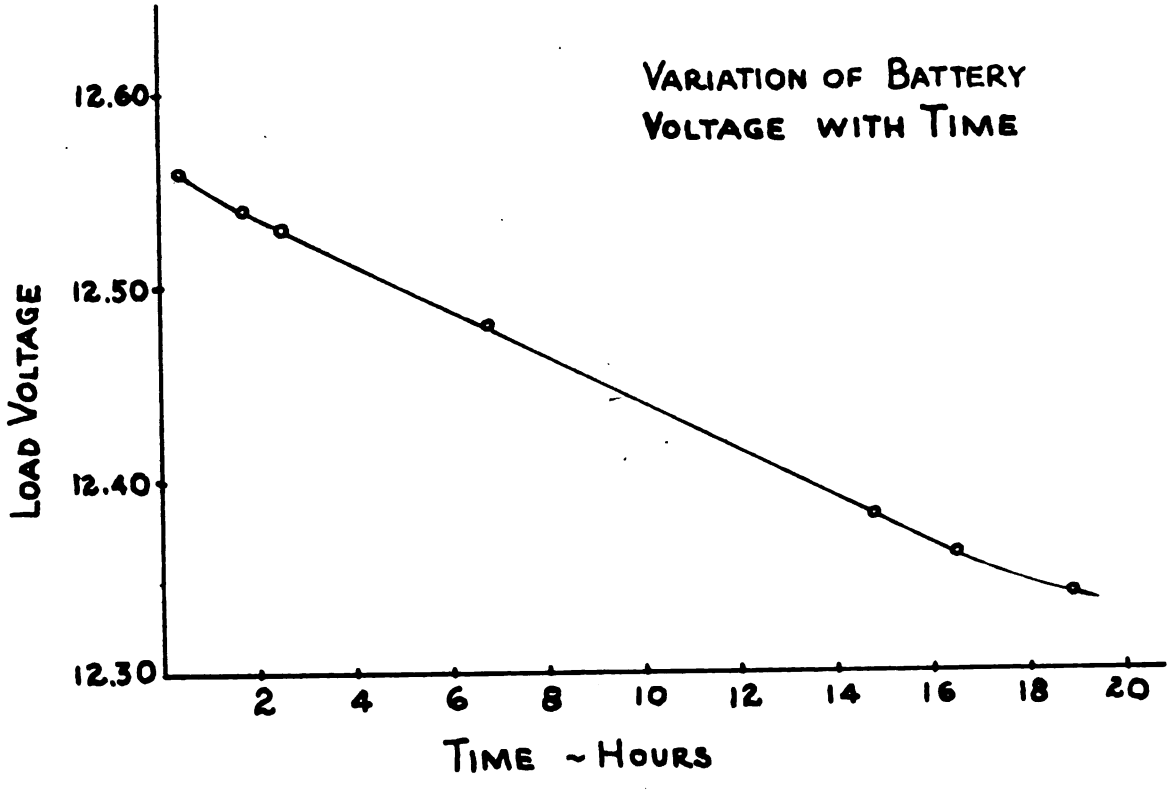
VARIATION OF BATTERY
VOLTAGE WITH TIME
LOAD VOLTAGE
12.60
12.50
12.40
12.30
2
4
6
8
10
12
14
16
18
20
TIME ~ HOURS

FIG. 4

TABLE I

FILAMENT CURRENT	PLATE CURRENT	SPACE GRID CURRENT
78 ma.	17.4 μa.	10.7 μa.
80	27.4	16.5
82	38.	24.
84	54.5	36.1
86	75.	54.7
88	103.	77.
90	138.	111.

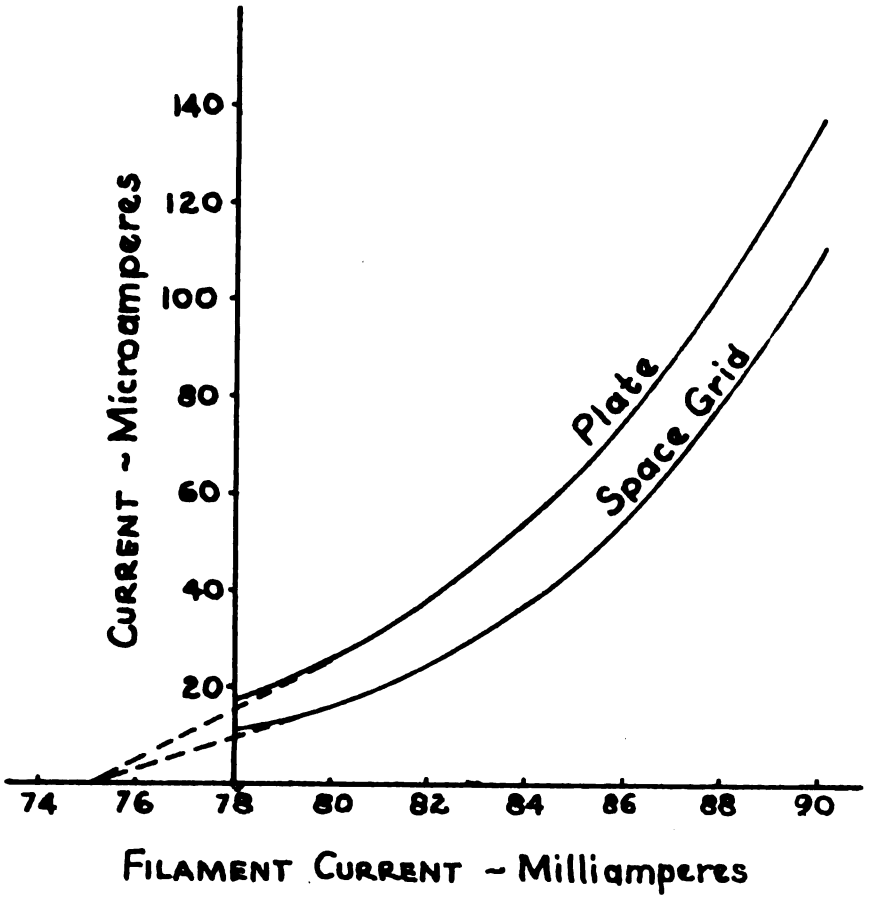

TYPE FP-54 TUBE

Plate - 8 Volts
Grid - -4 Volts
Space Grid - 6 Volts

FIG. 5

remain undisturbed by a variation in filament current (I_f), all other voltages remaining constant, we must have the condition fulfilled also that

$$R_p \frac{\partial I_p}{\partial I_f} = R_s \frac{\partial I_s}{\partial I_f} \qquad (2)$$

These two conditions will be satisfied only at that value of filament current at which the tangents to the curves in Fig. 5 have the same ratio as the ordinates. This will occur when the tangents to the two curves intersect on the I_f axis. With the operating data given in Fig. 5 the proper filament current would be slightly less than 80 milliamperes. Since the curves are relatively flat, for changes in filament current up to about one percent the curve and its tangent are essentially the same and variations of filament current up to this limit will have little effect upon the balanced circuit. This eliminates one of the most troublesome difficulties encountered in the amplification of small direct currents. In fact, with the conventional amplifier circuits the drift of the galvanometer was so rapid as to prevent any attempt to use the circuits experimentally. It might be noted here also that this compensation is effective for gradual changes which occur in the emissive characteristics of the filament. This is of especial importance in problems which require a considerable interval of time to elapse between the initial and final readings.

The operation of the apparatus is easily seen from Fig. 6. The filament current is determined by R_1. R_2 adjusts the potential on the plate and on the space charge grid. R_s and R_p are the two external arms of the bridge as previously mentioned. R_f is for the purpose of applying the correct potential to the space charge grid.

R_4 controls the sensitivity of the galvanometer. R_5 was for the purpose of applying a fixed bias to the control grid but was not used. R_6 is used to set the voltage across the potentiometer to the proper voltage to make it direct reading in volts.

To set the apparatus in operation the constants are set at their approximate values (Fig. 6). For this information and much excellent advice, credit must be given to a very thorough paper on thermionic amplifiers by MacDonald.[5] After being allowed an hour or so of warming up to enable the temperature distribution in the FP-54 to reach a steady state the apparatus is ready for adjustment. For the preliminary adjustments the galvanometer is replaced by a microammeter. First R_p is set for zero current through the meter. The filament current is then varied slightly by means of R_1, which will unbalance the system unless, as is very seldom the case, the system happens to be adjusted to fulfill the conditions outlined previously for the compensation of the balance with respect to the filament current changes. The circuit is rebalanced by another adjustment of R_p. This process is repeated again and again until a value for R_p and R_1 is found for which the circuit is balanced and remains that way even for slight variations of R_1. The galvanometer is then returned to the circuit and a final adjustment of the system is made. The circuit will now be sensitive only to variations of the potential on the control grid and is ready for operation.

In the grid circuit the photoelectric cell, a small battery, and the potentiometer are placed in series and connected to the grid and ground or filament. Preliminary work was done with a conventional high resistance, 10^{12} ohms or greater, connected

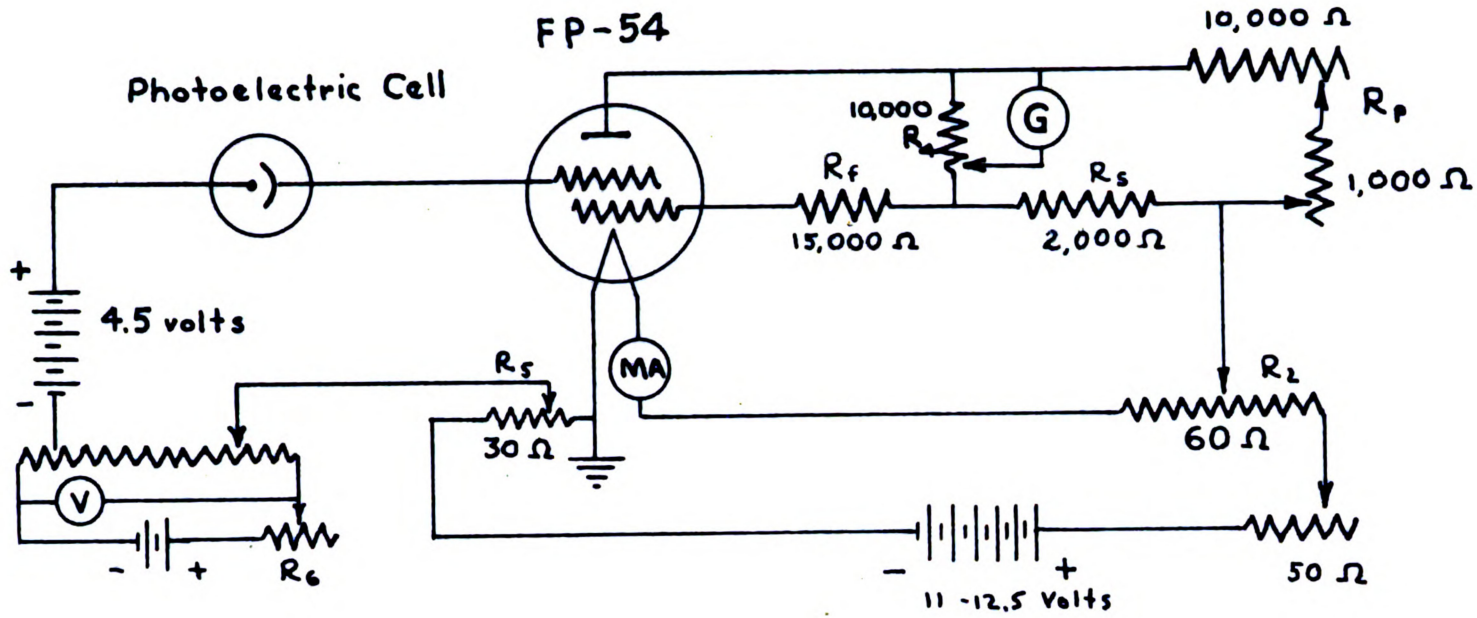

CIRCUIT DIAGRAM

FIG. 6

from the control grid to the negative post of the 4.5 volt battery. The voltage across this resistor depends linearly, if Ohm's law holds, upon the photoelectric current and hence is a function of the illumination. It was found in this particular set-up, however, that the removal of this resistor improved the operation and sensitivity of the amplifier. The actual behavior of the grid circuit is as follows: An insulated grid in a vacuum tube will reach an equilibrium potential, negative, which repels all further electrons emitted from the filament, or, if there is some current leakage, the electrons which do reach the grid carry the same charge as leaks off during the interval of time considered. In this circuit the photoelectric cell has a dark current which, although under ordinary applications is negligible, is of considerable magnitude compared to the true photoelectric currents being measured. (Information supplied by Dr. G. K. Green of the University of Illinois). This current caused the difficulty with the resistors in the circuit. The current was so large that practically the entire voltage of the battery was across the resistance at zero illumination, leaving no additional potential available to be impressed upon the grid. With the resistor removed, the action depends upon the variation of the dark current and the photoelectric current with the voltage across the cell. This variation of current with voltage is shown graphically in Fig. 7. When the cell is illuminated there is an increase in the current flowing through the cell. This effectively decreases the potential of the grid by draining off charge faster than it comes on from the filament. The change of grid potential, of course, unbalances the bridge and there is a galvanometer deflection. The

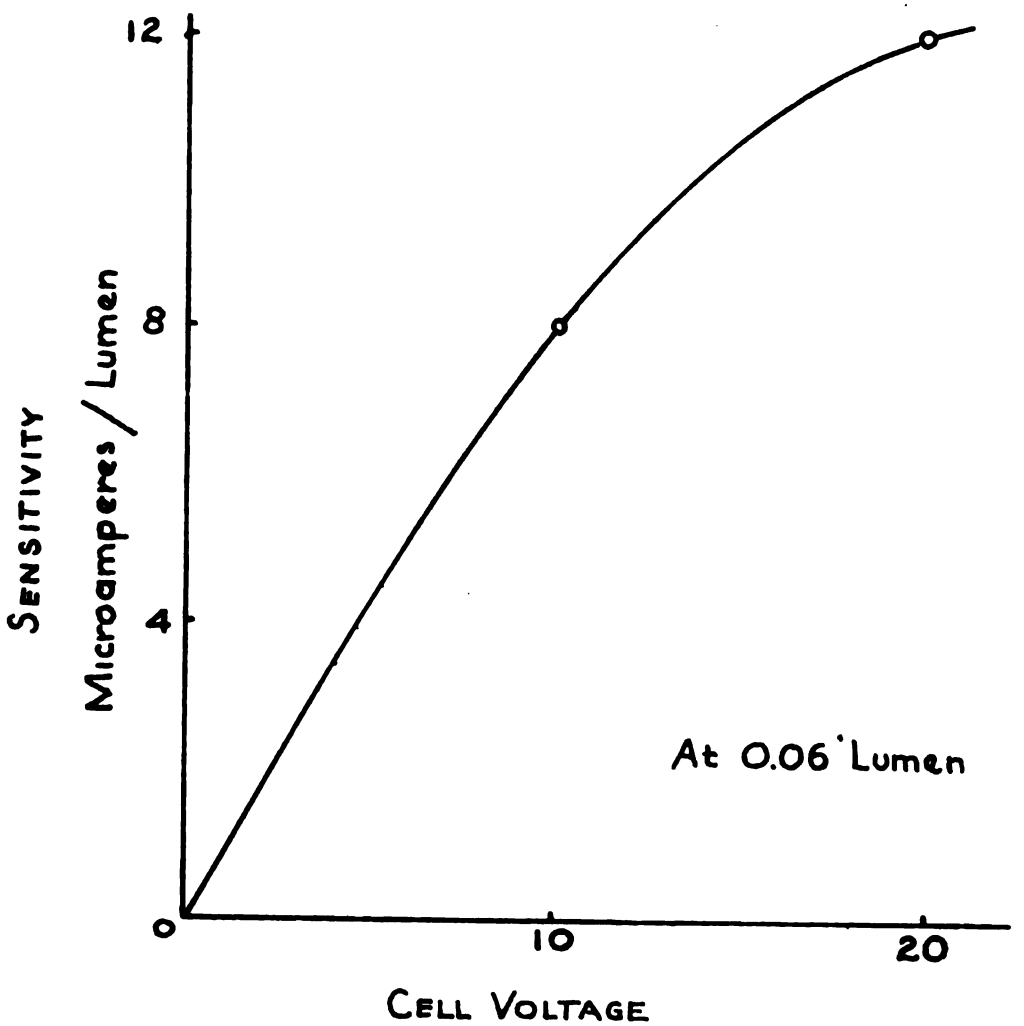

Photo Cell Response

Fig. 7

galvanometer can be returned to zero only by returning the grid to its original potential which in turn can be done only by restoring the current flowing from the grid through the cell to its original value. By means of the potentiometer an E.M.F opposing the E.M.F of the 4.5 volt battery is introduced into the circuit. This lowering of the potential across the photoelectric cell reduces the sensitivity of the cell until the original condition is reached at which time the voltage introduced is read directly from the potentiometer scale.

The amplifier was used as a null instrument in which the galvanometer reading and hence the control grid voltage were kept constant and the intensity readings were made from the potential required at the potentiometer to keep the bridge circuit balanced. It was possible with this system to use the most sensitive galvanometer available, a Leeds and Northrup type HS-2290 which has a specified sensitivity of 10^{-11} amperes per millimeter at a scale distance of one meter. The mechanical sensitivity of the instrument was so great that it was necessary to mount it on a shelf attached directly to the heavy foundation of the building in order to eliminate a constant mechanical vibration of such magnitude that the scale could not be read. Residual vibrations were further damped by setting the galvanometer on a heavy iron disc supported by sponge rubber pads. The solidity of this mounting made possible a rather long optical arm, about four meters, which was the maximum length possible in the room. At this distance a change in potential of one thousandth of a volt on the control grid caused a deflection of about one millimeter on the galvanometer scale which was ample to permit the potentiometer to be read to thousandths of a volt. The

light source for the galvanometer was a 32 c.p. automobile headlight bulb. An image of its filament was formed on the mirror of the galvanometer by a single lens which was mounted with the lamp in a housing especially designed to eliminate stray light. A long focus lens directly in front of the galvanometer formed, by means of the reflected light, an image of the projection lens, and a cross-hair stretched across it, on a translucent screen upon the operating table. A pointer was attached to the screen in such a way that the light from the galvanometer mirror cast a sharp pointed shadow of it. The operator's task was merely to keep the image of the cross-hair on the pointer by manipulating the potentiometer while the photoelectric cell moved across the pattern.

To insure that the galvanometer was operating near its maximum sensitivity it was connected into a resistance network as shown in Fig. 8. The deflection of the galvanometer was 470 mm. which amounts to a sensitivity of 1.07×10^{-11} amperes per millimeter. This, because of the long optical arm, amounts to but one fourth the specified sensitivity, but being sufficient it was not thought worthwhile to tinker further with the delicate instrument.

Calibration Of The Photoelectric Cell and Amplifier

The inverse square law was applied for calibration of the photoelectric cell and the associated amplifier, An optical bench was set up in front of the diffraction slit, which was opened to its full width where it had no effect. On the bench a light source was placed. This consisted of an automobile headlamp encased in two thicknesses of typewriting paper to make it a diffuse source and to

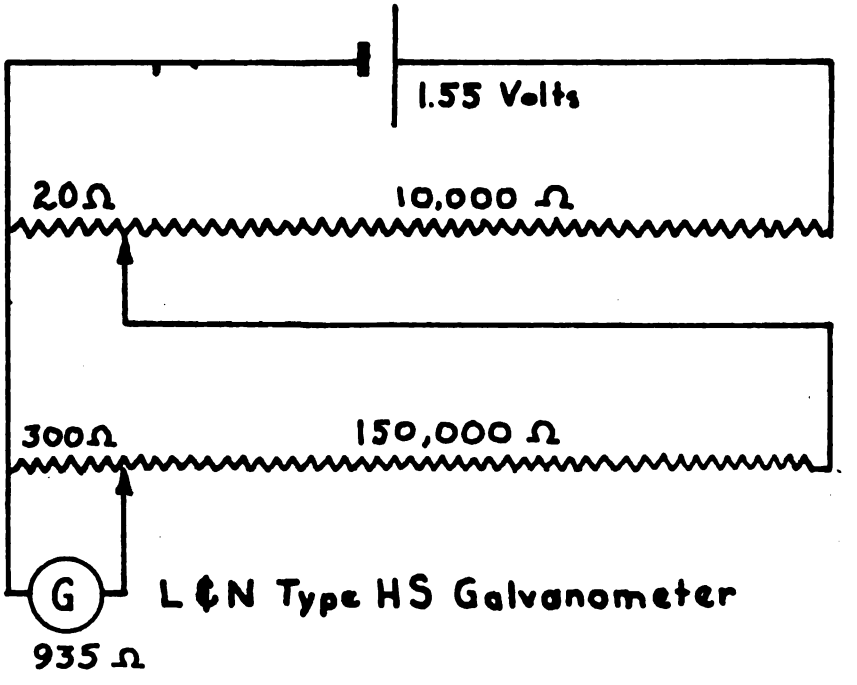

MEASUREMENT OF GALVANOMETER SENSITIVITY

FIG. 8

cut down its intensity. This was wrapped with opaque tape except for a small area of about one two hundredth of a square inch which served as the source. Directly in front of this were placed the same filters as were used with the light source for the diffraction pattern. The source and filters were arranged for convenient motion along the optical bench. Potentiometer readings were taken for various positions of the source on the optical bench. The area of the source and hence its intensity, was then changed and a new set of readings made. Four overlapping sets of data were taken in order to cover the necessary range of intensities. These data are recorded in Table II. They are plotted in Fig. 9. From this figure the comparative intensities of the sources were obtained. Since a given potentiometer reading indicates a particular intensity of illumination on the cell it is possible to equate the intensities of illumination produced by two of the sources in Fig. 9 when they produce equal potentiometer readings. By means of this Figure and the inverse square law the following relationships between the intensities of the four sources can be obtained:

$$I_{II} = (232.5^2/402.2^2)\ I_I$$

$$I_{III} = (231.3^2/378.5^2)\ I_{II}$$

$$I_{IV} = (426.5^2/218.5^2)\ I_I$$

I standing for intensity and the Roman subscripts for the number of the source as in Table III and Fig. 9. These relationships are adequate for the comparative measurements in which we are interested but in order to have an idea of the order of magnitude involved, a crude quantitative measurement of the intensity of source I was made. Because the intensity of this source was too small to be

TABLE II

DATA FOR CALIBRATION OF PHOTO-CELL AND AMPLIFIER:

Optical Bench Scale Reading	Total Distance From Cell To Source	Potentiometer Reading (Volts)
Source I		
	209.3 cms	.875
-8.0	269.5	.720
40.4	317.9	.618
81.3	358.8	.553
123.0	400.5	.502
151.9	429.4	.480
200.2	477.7	.440
Source II		
-8.0	269.5	.527
48.5	325.0	.422
122.8	400.3	.326
200.2	477.7	.266
Source III		
	209.3	.385
-8.0	269.5	.278
2.0	279.5	.278
28.2	305.7	.245
60.2	337.7	.214
75.9	353.4	.205
104.2	381.7	.200
129.9	407.4	.136
145.7	423.2	.131
200.0	477.5	.133
Source IV		
	209.3	1.175
-8.0	269.5	1.073
39.5	317.0	.995
90.7	368.2	.920
135.1	412.6	.865

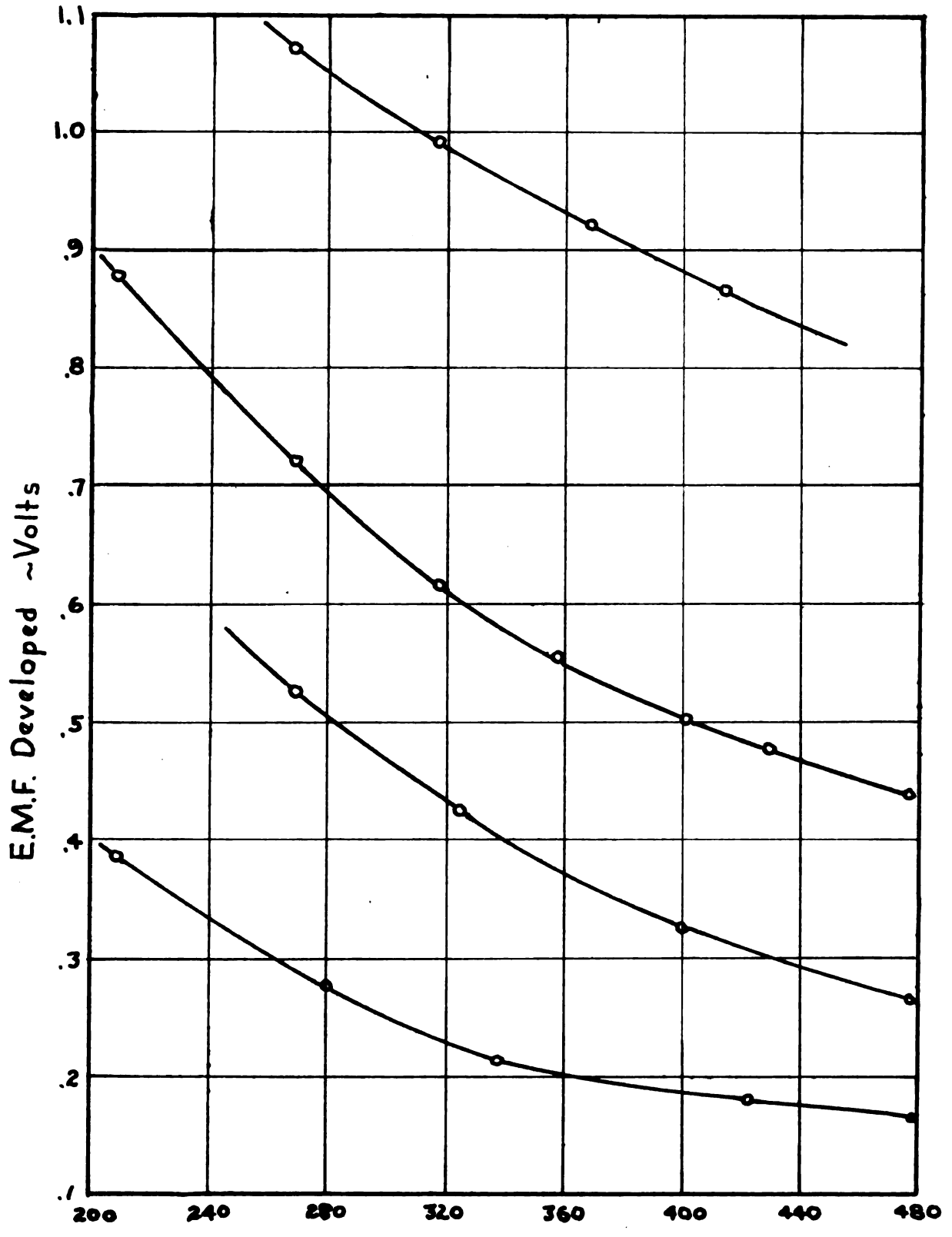
1.1
1.0
.9
.8
.7
.6
.5
.4
.3
.2
.1
E.M.F. Developed ~Volts
200
240
280
320
360
400
440
480
Distance from Photo Cell ~Cms.

FIG. 9

read on an ordinary illumination meter, an intermediate standard was necessary. For this purpose an ordinary candle was chosen. It gave an illumination of seven foot candles when ten cms. from the illumination meter which corresponds to an intensity of .75 candles for the candle. This value is subject to an error of about 4% due to deviations from the inverse square law at this distance because of the finite size of the photovoltaic cell of the meter and of the flame of the candle.

Source I was then compared with the candle by means of a grease-spot photometer with the following result:

$$I_I/15^2 = .75/185^2$$

$$I_I = .005 \text{ cp.}$$

In order to take full advantage of significant figures, assume Source I as .00500 cp. and from the relationships previously given:

$$I_I = .00500 \text{ cp.}$$

$$I_{II} = .00247 \text{ cp.}$$

$$I_{III} = .00092 \text{ cp.}$$

$$I_{IV} = .0190 \text{ cp.}$$

Using these intensities and Table II the illumination on the cell for each reading of the potentiometer can be calculated by means of the equation: Illumination $= \frac{KI}{d^2}$ lumens/cm^2 where K = 1 when d is in cms. From which comes Table III.

This table is plotted in Fig. 10. Note that inasmuch as the potentiometer was set to a reading of 0.100 volts at no illumination, this value has been subtracted from the potentiometer readings of Table III before plotting. A large plot of this graph was used as the calibration curve for conversion of potentiometer

TABLE III

Illumination Lumens/cm^2	Potentiometer Reading (volts)
4.03×10^{-9}	.163
5.14	.181
5.54	.186
6.30	.200
7.36	.205
8.07	.214
9.85	.245
10.83	.263
11.8	.278
12.7	.278
15.4	.326
21.0	.385
23.4	.422
21.9	.440
27.1	.480
31.2	.502
34.1	.527
38.9	.553
49.5	.618
68.9	.720
111.8	.865
114.2	.875
140.3	.920
189.3	.995
261.6	1.073
433.5	1.175

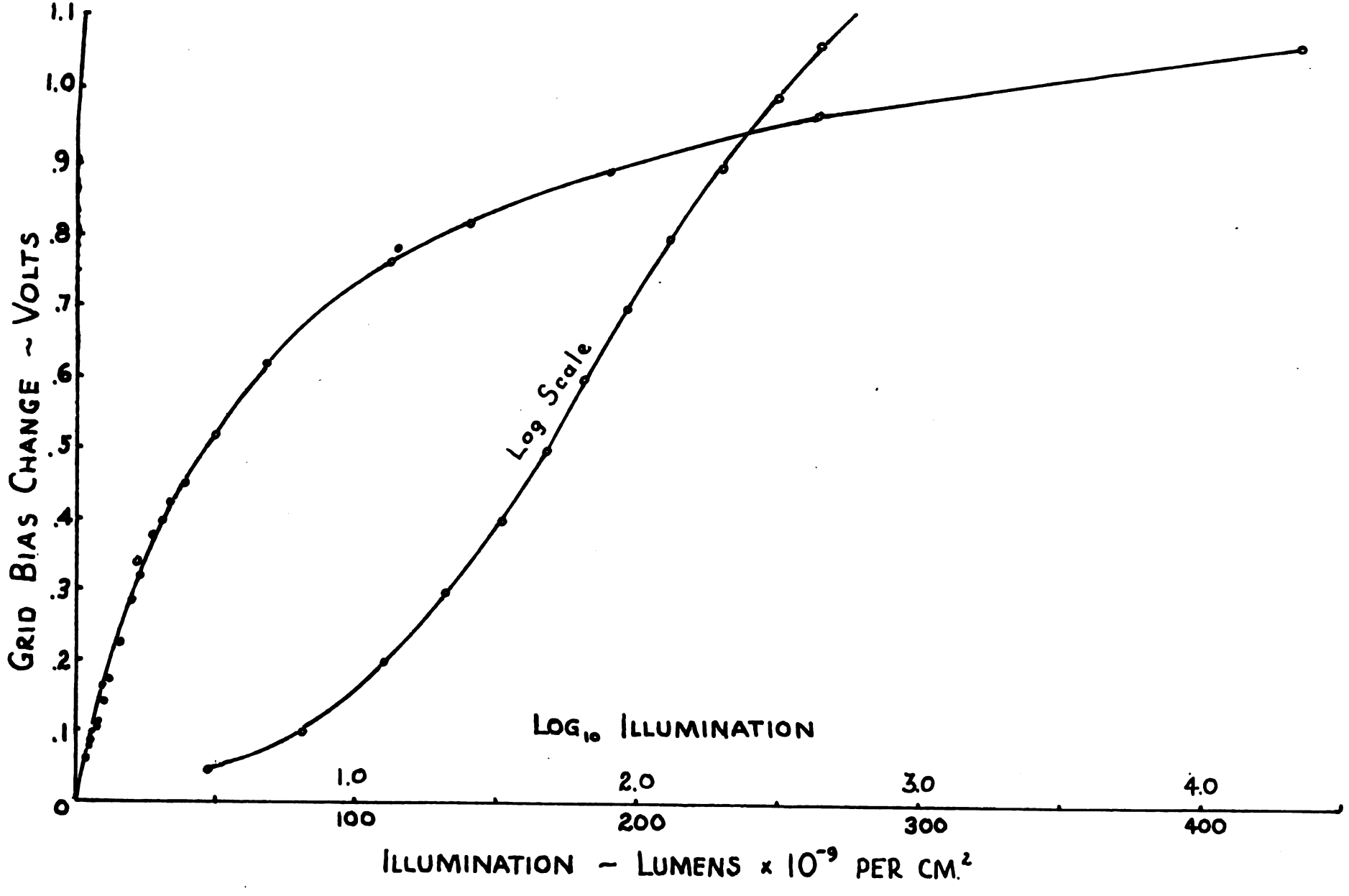
Grid Bias Change ~ Volts
1.1
1.0
.9
.8
.7
.6
.5
.4
.3
.2
.1
0
Log Scale
Log10 Illumination
1.0
2.0
3.0
4.0
100
200
300
400
Illumination ~ Lumens x 10-9 per cm.2

Fig. 10

readings to intensities in the analysis of the diffraction pattern. The nearly logarithmic response of the amplifier at the higher intensities is notable.* This can be seen in Fig. 10 where the grid bias change was plotted also against the logarithm of the intensity to facilitate an extrapolation at the high intensity end of the curve.

Measurement of Diffraction Patterns

Preliminary measurements revealed the usual array of experimental "bugs." The galvanometer would make frequent large and often permanent jumps, there was a constant drift of the zero point, and various minor perturbations were present. The exact causes of the difficulties were never determined but their magnitudes were reduced to a nearly negligible amount by a thorough shielding of the components and careful soldering of every connection possible. The remaining connections were carefully cleaned and made tight. The potentiometer and galvanometer, only, were unshielded. The potentiometer, being at ground potential, was placed outside of the shielded control box. The galvanometer would have been better if shielded but by twisting the leads to it and removing them as far as practical from the operator, the capacitance

*Attention has been called to a paper on this subject which has appeared since this work was completed.[6] This type of circuit is shown theorectically to give a truly logarithmic response of plate current to illumination of photoelectric cell under the conditions that the ohmic current in the grid circuit is small compared with the photoelectric current and that the load resistance of the plate circuit is large, on the order of one megohm. Deviations from these two conditions and the fact that the plate current is maintained constant in a bridge circuit operated as a null instrument prevents the realization of this ideal condition.

changes due to motions of the operator had very slight effects. Needless to say, careful adjustment of the balance circuit was a necessity.

It was necessary to make a dozen measurements of the pattern before the difficulties were eliminated sufficiently to give an acceptable set of measurements. The data for one of the earlier and the last two pattern are tabulated in Table IV. They are listed as patterns I, II, and III respectively. These data are plotted in Fig. 11.

Pattern I shows the erratic early behavior of the apparatus. There are numerous discontinuities in the curve and a marked tendency exists for the galvanometer to remain at each reading rather than follow the pattern. This was probably due to a slight rubbing in the galvanometer. Pattern II was taken with the carriage traveling in the opposite direction to its motion in Pattern I. The play in the screw is very noticeable in the displacement of the peaks. Pattern III is the one which was used and is a smooth curve except for two points in the very low ranges which are obviously errors. This pattern is plotted alone in Fig. 12 where it has been plotted on both sides of its axis of symmetry although the data does not extend much beyond the first maximum on one side.

By means of the calibration curves (Fig. 10) the data for this curve have been translated into actual intensity values and these values (which are given in the sixth column of Table IV) have been plotted in Fig. 13. This figure gives the relative intensities of the different portions of the curve in their true relation as measured. Comparison of this figure with Fig. 12 reveals the merit

TABLE IV

Scale Reading (inches/2)	Potentiometer Readings (volts)			Voltage Change III	Intensity Lumens/c.m.^{2} x 10^{-9}	Distance from center of III (inches)
	Pattern I	Pattern II	Pattern III			
2.000	.100					
3.000	.100					
3.600			.100	.000	.000	
3.700	.100					
3.800	.100		.103	.003	.2	
3.900	.174					
4.000	.183					
4.100	.215		.110	.010	.65	
4.200	.215		.135	.035	2.3	
4.300	.157					
4.400	.190		.135	.035	2.3	
4.500	.190		.135	.035	2.3	
4.600	.157		.120	.020	1.3	
4.700	.145		.106	.006	.4	
4.800	.177		.129	.029	1.9	
4.900	.177		.140	.040	2.5	
5.000	.205		.145	.045	2.8	
5.100	.212		.145	.045	2.8	
5.200	.225		.164	.064	4.0	
5.300	.236		.131	.031	2.0	
5.400	.236		.131	.031	2.0	
5.500	.236		.160	.060	3.8	
5.600	.292		.180	.080	5.0	

Scale Reading (inches/2)	Potentiometer Readings (volts)			Voltage Change III	Intensity Lumens/cm.² x 10⁻⁹	Distance from Center of III (inches)
	Pattern I	Pattern II	Pattern III			
5.700	.328		.200	.100	6.3	
5.750	.328					
5.800	.308		.215	.115	7.0	
5.900	.308	.171	.211	.111	6.8	
5.950	.285	.171				
6.000	.285	.185	.200	.100	6.3	
6.050	.249	.200				
6.100	.260	.265	.261	.161	10.7	
6.150	.347	.300				
6.200	.395	.367	.310	.210	13.8	.500
6.300	.488	.395	.410	.310	21.8	.450
6.350	.518	.455				
6.400	.538	.418	.475	.375	24.6	.400
6.450	.538	.378				
6.500	.507	.355	.475	.375	24.6	.350
6.550	.476	.345				
6.600	.477	.478	.311	.211	13.9	.300
6.650	.449	.663				
6.700	.585	.800	.405	.305	21.5	.250
6.750	.756	.935				
6.800	.900	1.057	.770	.670	80.3	.200
6.850	1.016	1.120				
6.900	1.126	1.184	1.035	.935	224.	.150
6.950	1.187	1.210				

Scale Reading (inches/2)	Potentiometer Readings (volts)			Voltage Change III	Intensity Lumens/cm.^{2} x 10^{-9}	Distance from Center of III (inches)
	Pattern I	Pattern II	Pattern III			
7.000	1.284	1.248	1.178	1.078	440.	.100
7.050	1.262	1.252				
7.100	1.271	1.260	1.258	1.158	590.	0.050
7.150	1.295	1.246				
7.200	1.285	1.242	1.272	1.172	800.	.000
7.250	1.267	1.195				
7.300	1.242	1.150	1.258	1.158	690.	
7.350	1.187	1.047				
7.400	1.146	1.000	1.180	1.080	485.	
7.450	1.068	.885				
7.500	.999	.734	1.000	.900	240.	
7.550.	.877	.590				
7.600	.725	.550	.785	.685	84.	
7.650	.663	.500				
7.700	.456	.300	.430	.330	24.	
7.750	.414	.315				
7.800	.450	.370	.390	.290	21.	
7.850	.490	.372				
7.900	.536	.415	.500	.400	31.	
7.950	.536	.437				
8.000	.530	.400	.500	.400	31.	
8.050	.500					
8.100	.485	.265				
8.150	.451					

Scale Reading (inches/2)	Potentiometer Readings (volts)			Voltage Change III	Intensity Lumens/sq. cm. x 10^{-9}	Distance from Center of III (inches)
	Pattern I	Pattern II	Pattern III			
8.200	.420	.180				
8.250	.366					
8.300	.350					
8.350	.350					
8.400	.350					
8.450	.340	.168				
8.500	.200					
8.550	.213					
8.600	.224					
8.650	.224					
8.700	.224	.168				
8,750	.287					
8.800	.300					
8.850	.300					
8.900	.292					
8.950	.280					
9.000	.275					
9.150	.269					
9.200		.100				
9.250	.269					

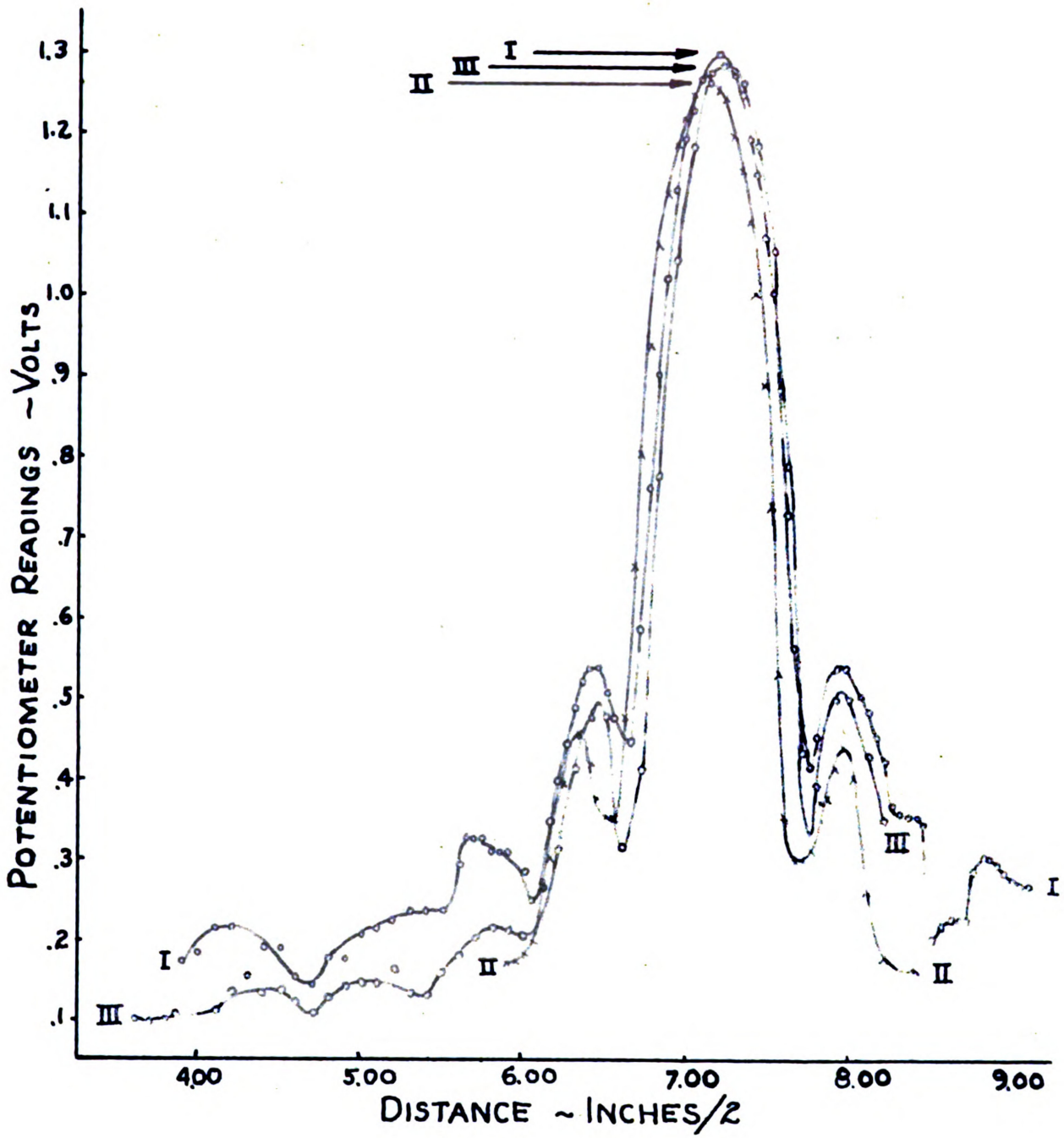
POTENTIOMETER READINGS ~ VOLTS
1.3
1.2
1.1
1.0
.9
.8
.7
.6
.5
.4
.3
.2
.1
I
II
III
4.00
5.00
6.00
7.00
8.00
9.00
DISTANCE ~ INCHES/2

FIG. 11

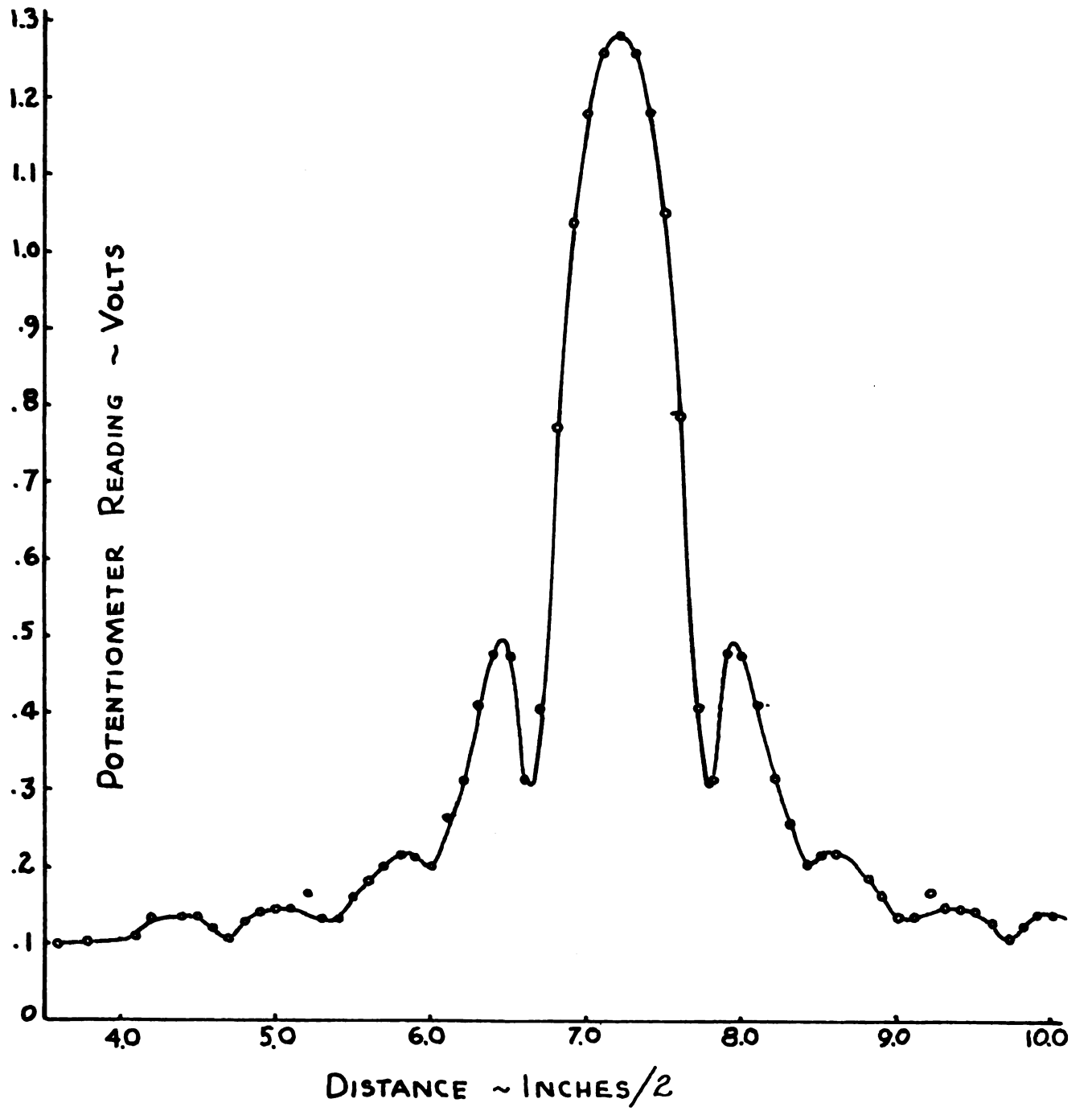
1.3
1.2
1.1
1.0
.9
.8
.7
.6
.5
.4
.3
.2
.1
0
POTENTIOMETER READING ~ VOLTS
4.0
5.0
6.0
7.0
8.0
9.0
10.0
DISTANCE ~ INCHES/2

FIG. 12

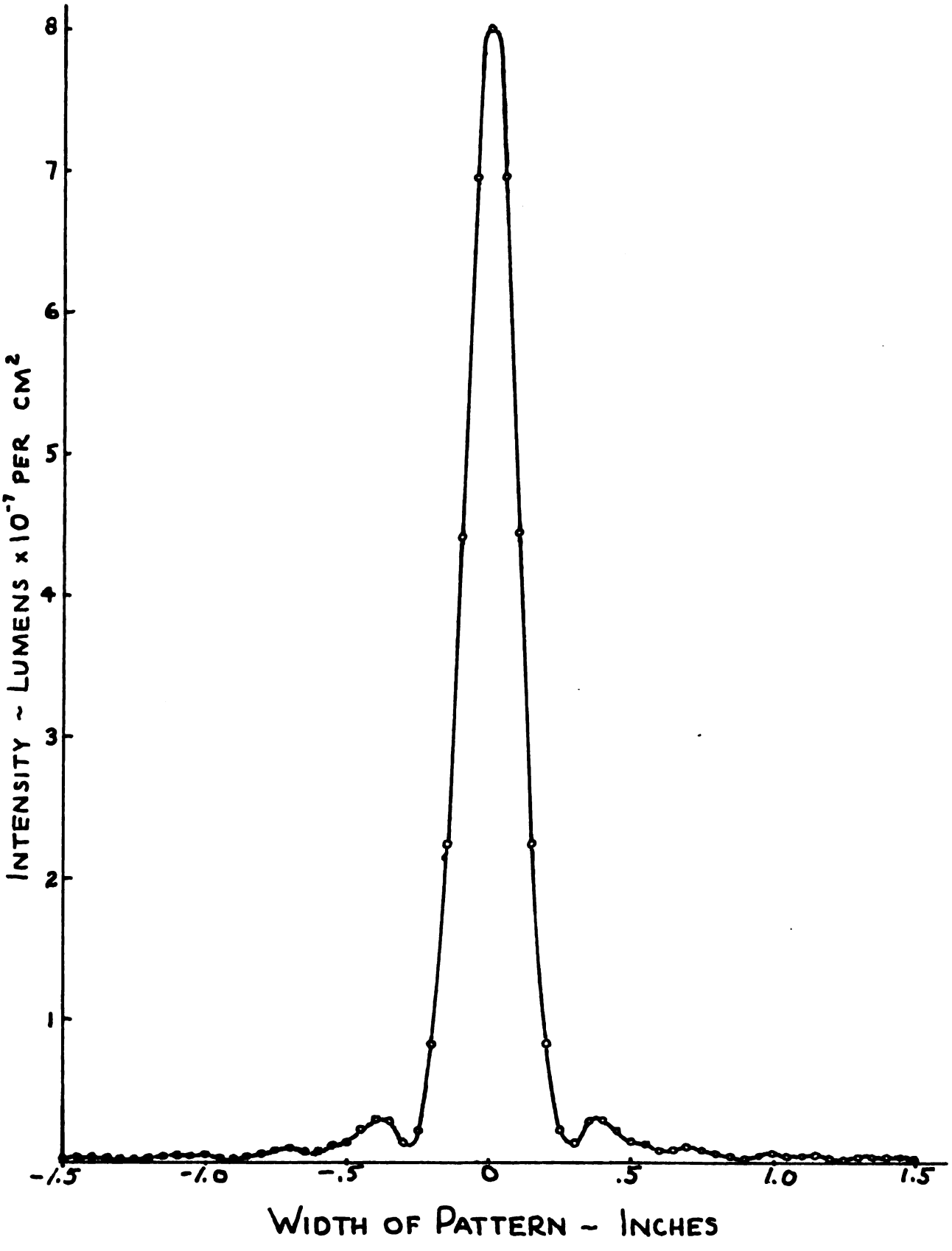
8
7
6
5
4
3
2
1
INTENSITY ~ LUMENS x 10⁻⁷ PER CM²
-1.5
-1.0
-.5
0
.5
1.0
1.5
WIDTH OF PATTERN ~ INCHES

FIG. 13

of an amplifier having the characteristics of the one used over one having a linear scale. Intensity variations which would be unrevealed by a linear amplifier stand out clearly in the measured pattern. The intensity curve (Fig. 13), however, is the one which must be compared with the theoretical pattern.

Comparison with Theoretical Values

Theory:

Fresnel's theoretical analysis of a pattern of this type consists of integrating over the wave front to find the resultant amplitude at any particular point, taking into consideration both amplitude and phase of the contribution from each differential area of the surface of the wave front. This derivation, in part or whole, can be found in any of the common textbooks of physical optics.

The process can be briefly sketched in a qualitative manner. Imagine a cylindrical wave front, shown in cross-section in Fig. 14. Let this wave front be divided into a large number of vertical strips, decreasing in width as the distance from the pole O increases in such a manner that the phase difference between corresponding parts of adjacent strips is constant for the waves reaching the point P from each point on the wave front according to Huygen's principle.

The resultant amplitude at the point P is the vector sum of the contributions of amplitude from each of the small strips. If the width of these strips is diminished to the limit of zero, the x and y components of the amplitude at P due to the wave surface between O and S are given by the Fresnel integrals

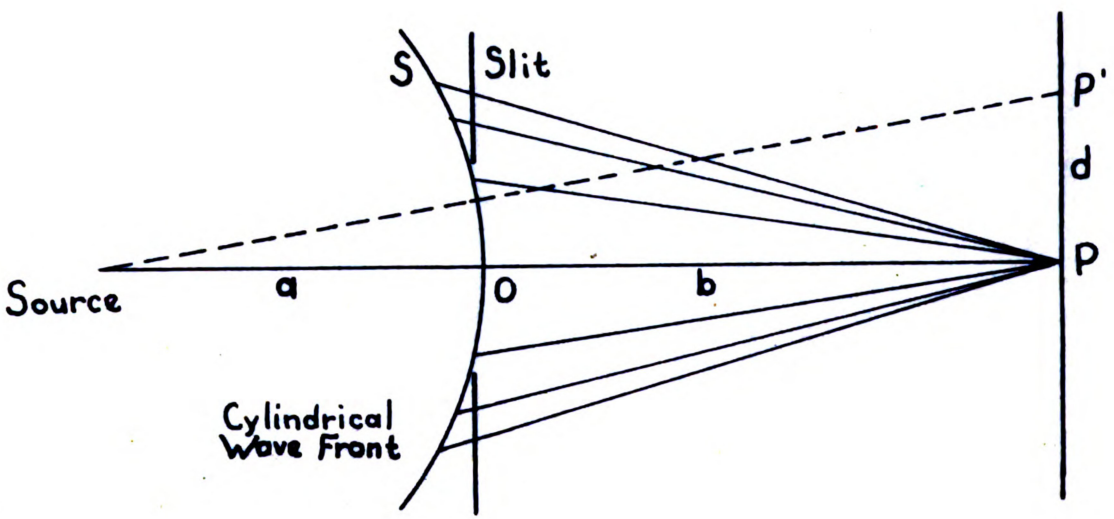

CROSS-SECTION OF CYLINDRICAL WAVE FRONT

FIG. 14

$$x = \int_0^v \cos \frac{\pi v^2}{2}\, dv \qquad (3)$$

$$y = \int_0^v \sin \frac{\pi v^2}{2}\, dv \qquad (4)$$

where s is the distance from O to S and

$$v = s\sqrt{2(a+b)/ab\lambda} \qquad (5)$$

The radius of curvature of the wave front and the distance from the pole to the point P are "a" and "b" respectively and have previously been given as 102 and 204 cms. respectively. The wavelength of the light is λ.

It may be noted that these integrals take no account of the obliquity factor $(1+\cos\theta)$ or the variation of the amplitude as the inverse of the distance from the source. For small angles these factors are both negligible, however. Several solutions of these integrals have been obtained. All, however, involve infinite series which converge more or less rapidly. If the values of x and y for various values of v are plotted the familiar Cornu spiral results. Fig. 15 is reduced from a large graph made from a table of these integrals.[6]

For a single slit diffraction pattern but a small section, Δs, of the wave front contributes to the pattern. For relatively small slits and distant sources Δs is equal to the width of the slit and corresponds to a distance Δv along the spiral given by

$$\Delta v = \Delta s\sqrt{2(a+b)/ab\lambda} \qquad (6)$$

If P is in a straight line with the source and the center of the slit, the relative intensity there can be found by measuring on the spiral the chord R, from $-\frac{\Delta v}{2}$ to $+\frac{\Delta v}{2}$. Now since the intensity of

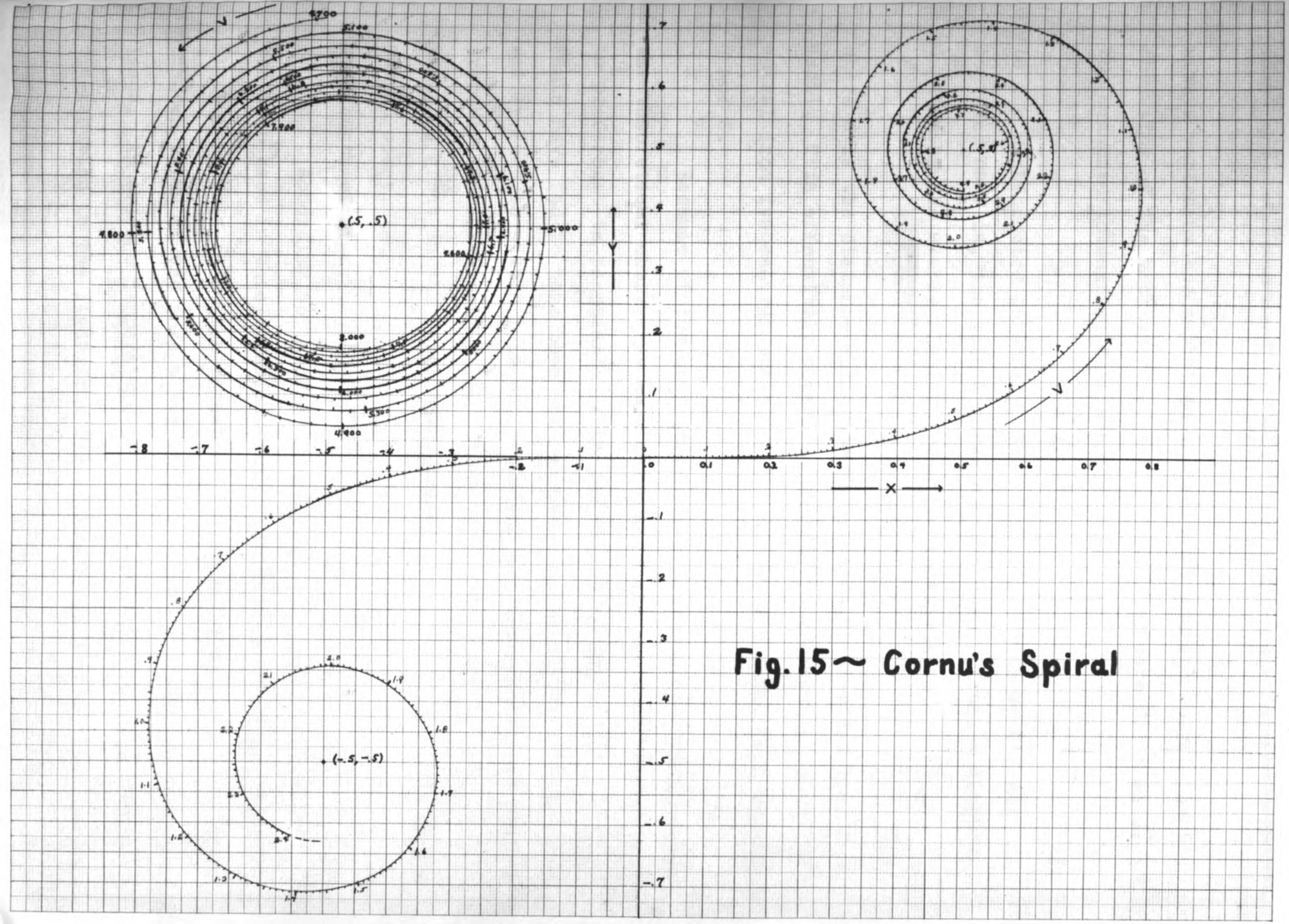

Fig. 15 ~ Cornu's Spiral

a wave varies as the amplitude squared (R^2) and the spiral gives the value of the amplitude for the unobstructed wave front as $\sqrt{2} = R_0$ the measured intensity, I, bears the relation

$$I = I_0 R^2/2 \qquad (7)$$

to the unobstructed intensity, I_0. For points such as P', not centered as P is, the pole O moves along the wave front a distance s given by the simple similar triangles relationship

$$s = d\ a/(a+b) \qquad (8)$$

where d is the distance along the screen from P, provided that d is small. This effectively moves the contributing length Δv along the spiral from its central position by a distance v found from equations 5 and 8.

Because of the many values of R to be determined in making the theoretical check they were taken from the original of Fig. 15 in preference to computation from the tables in which interpolations would have had to have been made anyway. Large values of R could be easily read to within $\pm$ 1% while for the smaller numbers the error probably did not exceed $\pm$ 5%. These errors will, of course, be twice as great in the calculated intensity because R is taken to the second power.

Wavelength of Light:

According to information supplied by the manufacturers the lamp used in this experiment operates at a temperature of 3025° Absolute. This is at the center of the filament and drops off to an unknown value at the ends where it is connected to the supporting leads. An average temperature of 3,000° was assumed. The energy distribution in the light from the filament was calculated from the

energy distribution in the radiation from a black body using Planck's formula

$$E_\lambda = \frac{8\pi hc}{\lambda^5\left(e^{\frac{hc}{\lambda kT}} - 1\right)} \qquad (9)$$

where E_λ is the energy in ergs per cm per unit volume and

$c = 3 \times 10^{10}$ the velocity of light

$h = 6.55 \times 10^{-27}$ Plank's constant

$k = 1.37 \times 10^{-16}$ Boltzman's constant.

TABLE V

λ	E_λ	λ	E_λ
7,000	3.13×10^3	6,000	3.74×10^3
6,000	2.20	5,000	1.11
4,000	3.11×10^2		

These data are plotted in Fig. 16.

The emissivity of tungsten was found to be linear in the visible range.[7] At 3,000° the values are

λ = 6650 A emissivity = .415

λ = 4670 A emissivity = .455

The data for the spectral sensitivity of the photoelectric cell and for the transmission characteristics of the filters were taken from curves supplied by the manufacturers. The filter characteristics are not all that could be desired. They are designed to isolate the mercury green line at 5460 A but do not give a very narrow region for an incandescent source. However, the intensity of the mercury line was not sufficient to make measurements of the pattern possible and the source chosen was a compromise between poor light and insufficient light.

Curve VI in Fig. 16 is the product of the transmission of

I Didymium Glass Filter Corning No. 512

II Yellow Shade Yellow Filter Corning No. 351

III Emissivity of Tungsten at 3000° K.

IV Spectral Response of Photoelectric Cell

V Energy Distribution in Black Body Radiation at 3000° K.

VI Effective Energy Distribution in Light Source

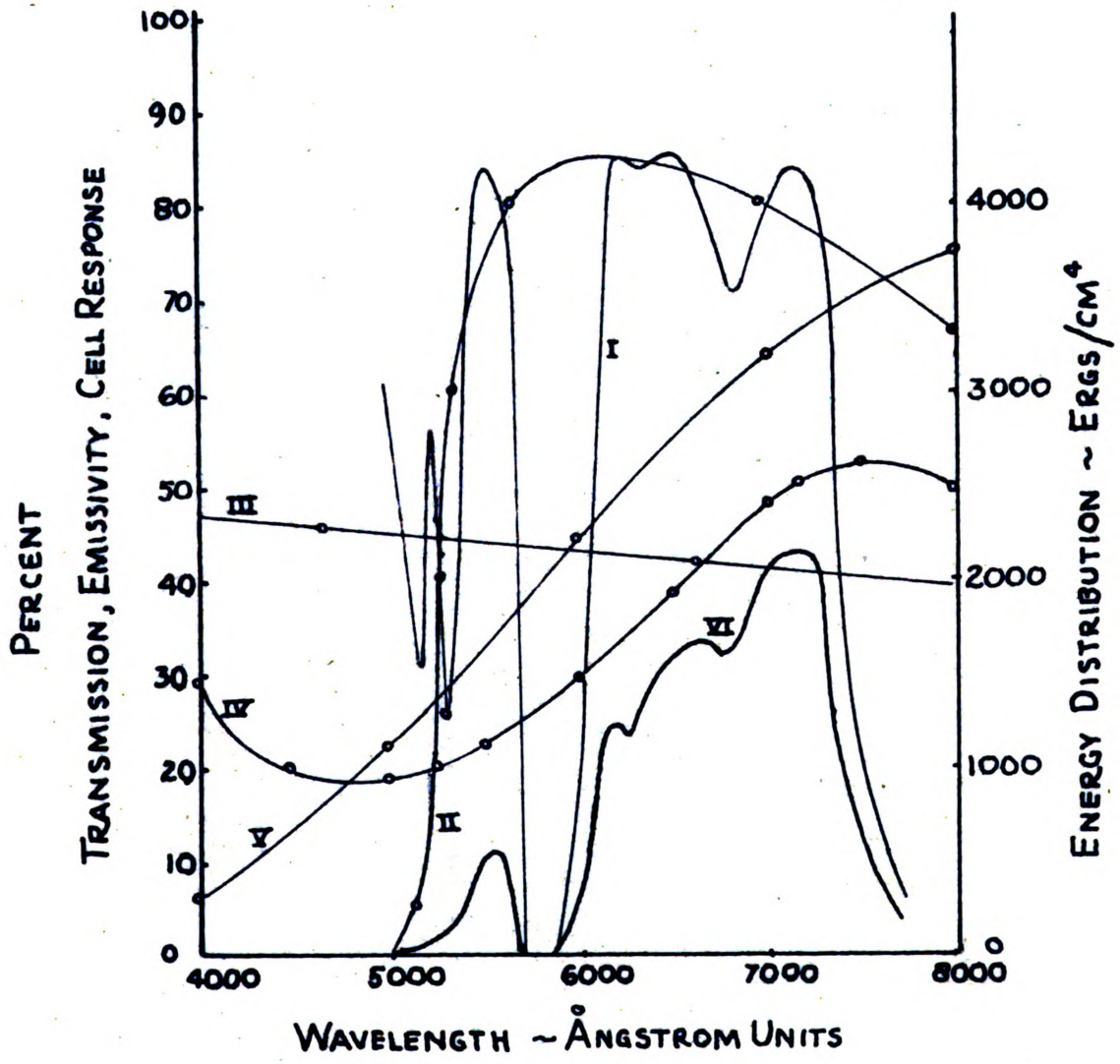

FIG. 16

the filter, the response of the cell, the emissivity of tungsten, and black-body radiation at 3,000°. It gives, in arbitrary units, the effective energy distribution in the filtered light as measured by the photo-electric cell.

Slit Width

Before the final calculations could be made a more accurate determination of the width of the diffracting slit had to be made. Previous experimenters have verified the application of Fresnel's integrals for the location of maxima and minima in the pattern. It is possible to make the calculation from data taken from Figs. 13 and 15. Figure 13 shows the first minimum to occur at 0.23 ± .01 inches or 0171 ± .025 cms. The average incident wavelength is seen from Fig. 16 to be at 6350 A ± 20 A.. Solving for v in equations (5) and (8) with these data we find that v = 4.9 ± .2 units of distance along the spiral. By inspection it is found that this corresponds to a Δv = .41± .01. The corresponding slit width is found from Eq. (6) to be 0.0137 ± .0005 cms.

Calculation of Theoretical Pattern

The theoretical pattern will be the sum of the patterns due to each wavelength present. Because of the large spread of wavelengths present, the ideal case was approximated by calculating patterns for wavelengths at intervals of 250 A. These patterns were then individually corrected for the relative amounts of energy they contained. That is each pattern was multiplied by a constant which was proportional to the area encompassed between the wavelengths 125 A on each side of the central wavelength and under the curve VI

TABLE VI

Distance Along Pattern		Intensity= kR^2	λ = 5550 v = .440		k = .56		λ = 6000 v = .420		k = .33	
Inches	cms	arbitrary	v	R	R^2	kR^2	v	R	R^2	kR^2
.000	.000	1.54	.000	.438	.192	.103	.000	.419	.176	.058
.025	.0637	1.53	.487	.433	.187	.105	.460	.413	.171	.056
.050	.1275	1.38	.973	.406	.165	.0925	.941	.392	.154	.051
.100	.254	1.01	1.943	.317	.100	.056	1.875	.320	.102	.034
.150	.381	.557	2.922	.197	.0388	.0217	2.812	.216	.0466	.01534
.200	.508	.205	3.896	.072	.00518	.0029	3.749	.063	.00397	.0023
.250	.635	.0358	4.870	.030	.00090	.00050	4.686	.021	.00044	.00023
.275	.6985	.0120	5.357	.024	.00440	.00230	5.155	.032	.00102	.00034
.300	.762	.0109	5.845	.086	.00722	.00405	5.624	.061	.00372	.00123
.350	.889	.0438	6.819	.093	.00865	.00485	6.561	.080	.00640	.00211
.400	1.016	.0650	7.795	.064	.00410	.00230	7.498	.054	.00292	.00221

λ = 6250 v = .412		k = 1.18		λ = 6500 v = .404		k = 1.55		λ = 6750 v = .396		k = 1.64	
v	R	R^2	kR^2	v	R	R^2	kR^2	v	R	R^2	kR^2
.000	.408	.166	.196	.000	.402	.162	.251	.000	.392	.154	.252
.459	.407	.166	.196	.450	.401	.161	.250	.443	.392	.154	.252
.922	.368	.151	.178	.904	.361	.145	.225	.890	.374	.140	.230
1.836	.321	.103	.121	1.801	.323	.104	.161	1.773	.331	.103	.169
2.755	.226	.0511	.0603	2.701	.233	.0543	.0841	2.659	.237	.0562	.0921
3.673	.120	.0144	.0170	3.602	.132	.0174	.0270	3.546	.145	.0210	.0344
4.591	.026	.00068	.00080	4.502	.040	.00160	.00248	4.432	.055	.00302	.00495
5.050	.017	.00029	.00034	4.952	.006	.00004	.00006	4.875	.020	.00040	.00066
5.509	.047	.00221	.00260	5.403	.033	.00110	.00170	5.319	.020	.00040	.00066
6.427	.034	.00706	.00833	6.303	.076	.00578	.00895	6.205	.068	.00462	.00758
7.346	.057	.00757	.00892	7.203	.087	.00757	.01173	7.092	.086	.00740	.0121

λ = 7000 v = .390		k = 1.99		λ = 7250 v = .382		k = 1.88		λ = 7500 v = .376		k = .75	
v	R	R^2	kR^2	v	R	R^2	kR^2	v	R	R^2	kR^2
.000	.388	.151	.300	.000	.381	.145	.272	.000	.375	.141	.106
.434	.387	.150	.299	.425	.380	.144	.271	.419	.373	.139	.104
.872	.372	.138	.274	.853	.365	.133	.250	.841	.359	.129	.0967
1.737	.320	.102	.203	1.699	.318	.101	.190	1.676	.318	.101	.0757
2.606	.242	.0586	.1166	2.549	.250	.0625	.118	2.515	.254	.0654	.0490
3.475	.156	.0243	.0484	3.399	.165	.0272	.0511	3.353	.172	.0296	.0222
4.343	.065	.00422	.00840	4.248	.061	.00656	.01232	4.191	.095	.00902	.00677
4.777	.0285	.00080	.00160	4.673	.046	.00212	.00398	4.610	.060	.00360	.00270
5.166	.0060	.00004	.00008	5.098	.011	.00012	.00023	5.029	.023	.00053	.00040
6.011	.058	.00336	.00669	5.947	.045	.00202	.00380	5.867	.035	.00122	.00091
6.949	.0825	.00680	.01353	6.797	.075	.00562	.01056	6.706	.069	.00476	.00358

of Fig. 16. These constants, k, the wavelength used, the values of v, Δv, R, R^2, kR^2, and hR^2 are tabulated in Table VI.

Correction for Width of Photo-electric Cell Slit:

The data of Table VI give the actual theoretical pattern. However, because of the finite width of the slit in front of the photo-electric cell, this pattern must be corrected before it is comparable with the measured diffraction pattern. This correction is made by plotting the theoretical curve (Fig. 17) and determining from the area under the curve the difference between the intensity at the center of the slit and the average intensity across the whole width of the slit. The corrections made are given in Table VII

TABLE VII

Distance Along Pattern - cms.	Correction	Corrected Intensity
.000	0	1.54
.0637	-.015	1.52
.1275	0	1.38
.254	0	1.01
.381	0	.557
.508	0	.205
.635	+.005	.0408
.6985	+.004	.0160
.762	+.003	.0138
.889	0	.0433
1.016	0	.0550

These corrected intensities need but to be put on the same scale as the measured intensities to be directly comparable with them.

Conversion To Same Scale:

If the measured and calculated patterns were identical the following relationship would hold:

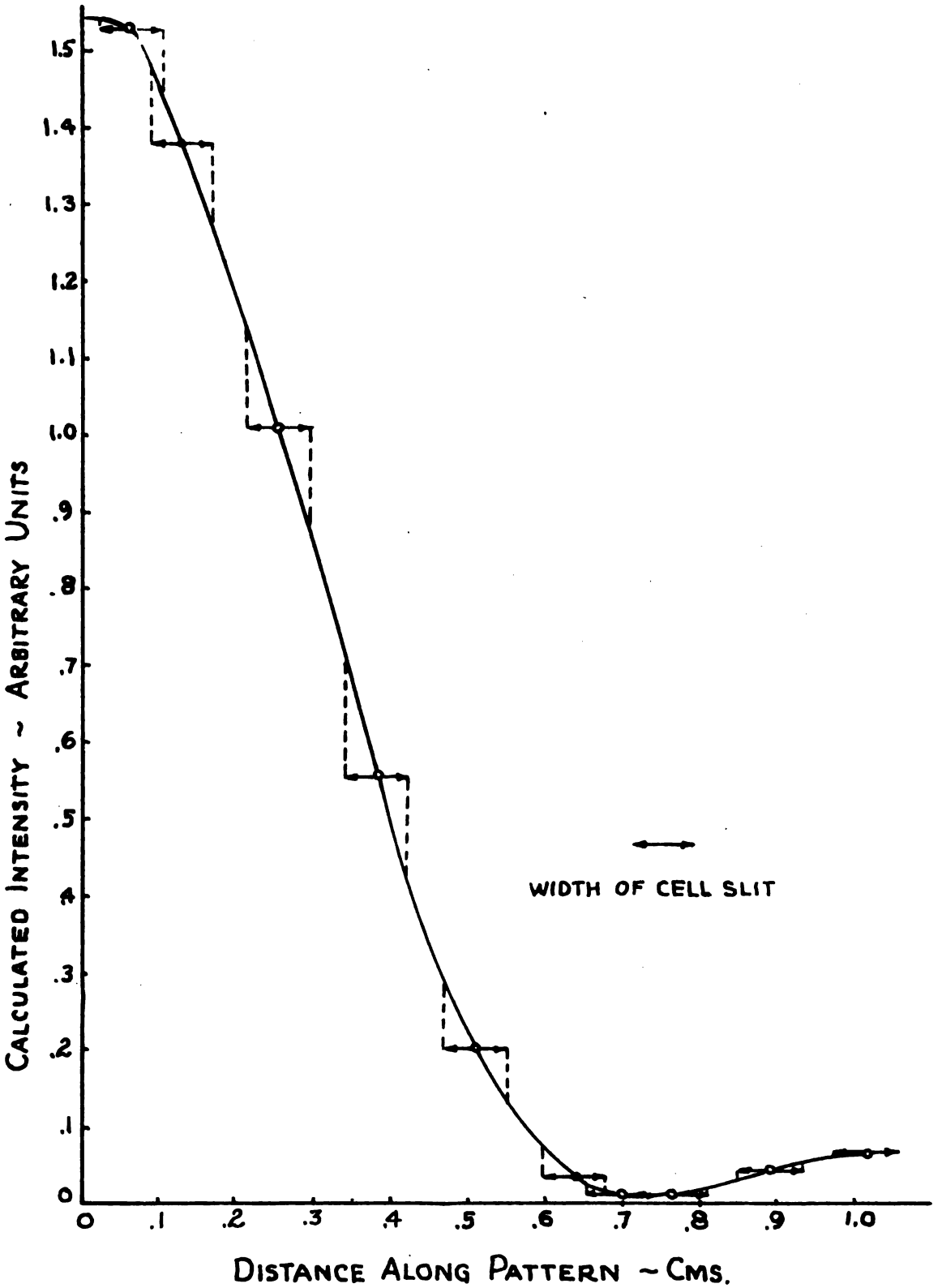
CALCULATED INTENSITY ~ ARBITRARY UNITS
1.5
1.4
1.3
1.2
1.1
1.0
.9
.8
.7
.6
.5
.4
.3
.2
.1
0
WIDTH OF CELL SLIT
0
.1
.2
.3
.4
.5
.6
.7
.8
.9
1.0
DISTANCE ALONG PATTERN ~ CMS.

FIG. 17

$$I_{meas.} = I_{calc.} \times k$$

where k is a constant to correct for the different units in which the two intensities have been measured. The ideal determination of k would come from the ratio of the two intensities at their maxima, since at this point the effect of the corrections and the frequency range of the light are a minimum. However, because this point on the measured curve was found from an extrapolation of the calibration curve, it will be necessary to use the first measurement made away from the maximum. This is at 0.050 inches or 0.1275 cms. The intensities are (from Tables IV and VI):

$$I_{meas.} = 6.90 \times 10^{-7}$$

$$I_{calc.} = 1.38$$

From these values $k = 5.00 \times 10^{-7}$. In the following summary of data the calculated intensities of Table VII have all been multiplied by k.

TABLE VIII

Distance Along Pattern From Center		Intensity Lumens/cm^2 x 10^{-7}	
Inches	Cms.	Calculated	Measured
.000	.000	7.70	8.00
.025	.0637	7.60	
.050	.1275	6.90	6.90
.100	.254	5.05	4.40
.150	.381	2.78	2.24
.200	.508	1.035	.707
.250	.635	.205	.215
.275	.6985	.010	
.300	.762	.070	.139
.350	.889	.212	.286
.400	1.016	.308	.286

The disagreement between the observed and calculated intensities is quite large, reaching a maximum of 50% for the minimum

intensities. However, the discrepancy does not appear quite so serious when the shapes of the patterns are plotted, as in Fig. 18.

Discussion of Errors

The errors in this experiment may be discussed under two heads: one the errors in the measured pattern and the other the errors in the calculated pattern.

In the measured pattern the distance along the pattern when read to the nearest scale division (1/100 revolution) was correct to ± .0005 inches. This is 1% of the smallest movement of the carriage which was made. By rotating the lead screw in one direction only during a measurement and by setting the dial with an accuracy of about 1/10 scale divisions the error was reduced to considerably less than one percent. The wear of the soft babbitt nut which was driven by the lead screw amounted to less than 0.0001 inches per revolution. This is, of course, negligible.

The potentiometer, when read to its nearest division, has an accuracy of ± .0005 volts. This is an error of 0.25% in the smallest reading which was used in the comparison of patterns and is proportionately smaller in the large values.

The calibration curve (Fig. 10) has somewhat less accuracy due to the taking of constants used in its calculation from a graph (Fig. 9). Except for two points the calibration curve is quite consistent. These two points, of which the poorest is in disagreement with the curve by 10%, may have been due to a small transient deflection of the galvanometer. Consideration of the distribution of the other points on the curve would indicate that the curve is not

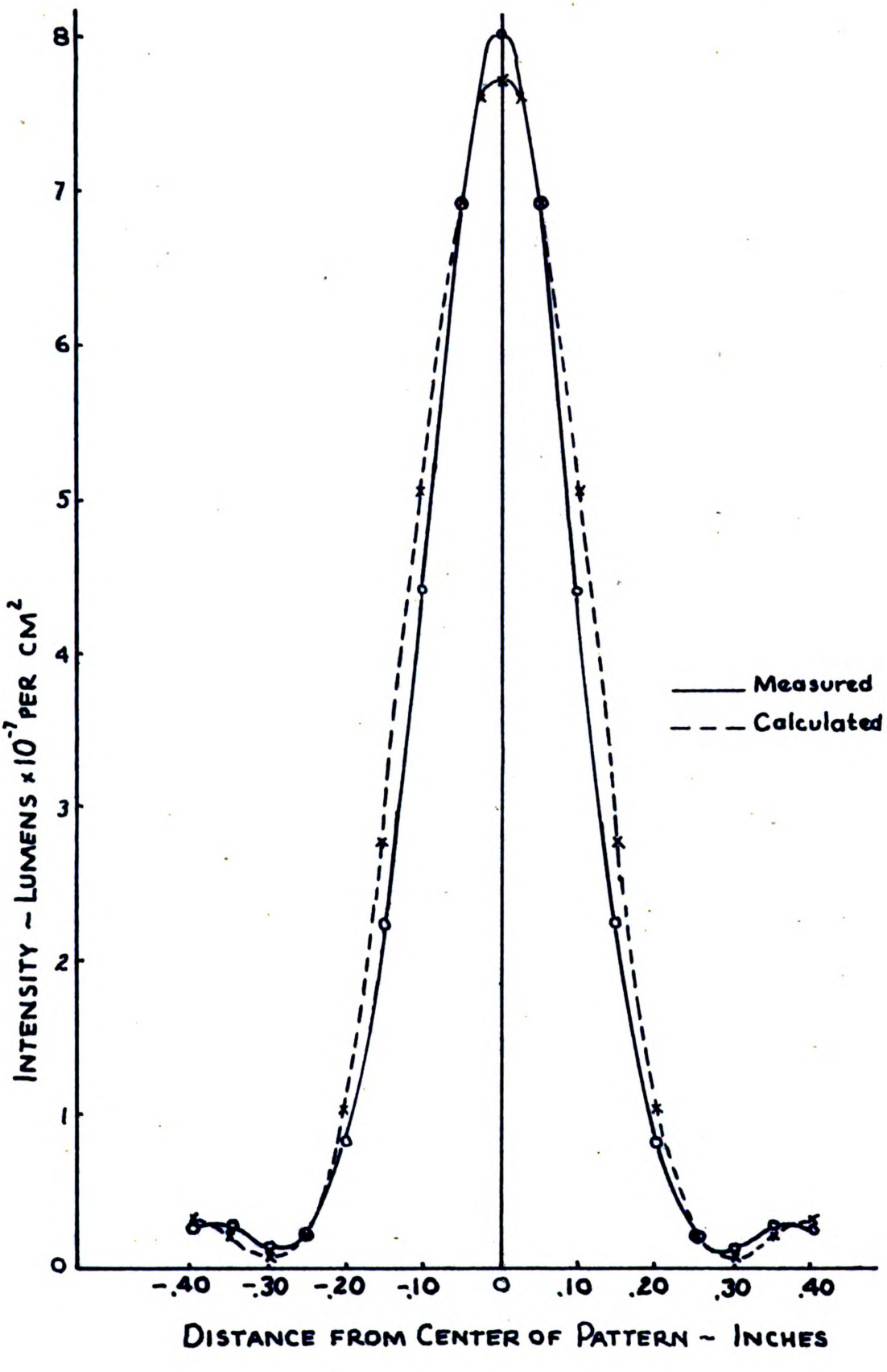
8
7
6
5
4
3
2
1
0
INTENSITY ~ LUMENS x 10⁻⁷ PER CM²
Measured
Calculated
-.40
-.30
-.20
-.10
0
.10
.20
.30
.40
DISTANCE FROM CENTER OF PATTERN ~ INCHES

FIG. 18

in error by as much as 5% at any point save the extreme value of Fig. 14 where the extrapolation may cause an error of as great as 7%.

The application of the potentiometer in the circuit used calls for a flow of current whereas a potentiometer is calibrated for and usually operated with no current flowing in its external circuit. But in this case the current flowing, the photoelectric current, is smaller than the least amount which would be detected in an ordinary circuit, and hence does not disturb the calibration of the potentiometer.

Drift of the galvanometer null point and transient deflections were carefully watched for in both the calibration and pattern measurements. In both cases the drift was reduced to a negligible amount while any transients were of small magnitude as evidenced by the few irregular points noted in Figs. 10 and 12.

No record was taken of the line voltage, which of course would affect both the calibration curve and the pattern. However, it was observed several times during the experiment and the fluctuations were barely enough to cause perceptible motion of the needle, a fraction of a volt. Furthermore, readings were usually taken late at night when the line load was essentially constant.

In the calculated pattern the wide range of wave lengths included in the light source necessitated numerous assumptions and approximations, most of them rather small in consequence, but resulting in a considerable over all uncertainty.

The first assumption, regarding the temperature of the filament, is of unknown magnitude. The average temperature is

probably somewhat less than the assumed value of 3,000° Absolute. This results in curve VI of Fig. 16 being distorted. Further distortion is introduced by the fact that the filters may not have exactly the transmission curves specified. Moreover, the distribution of the total energy among the eight patterns chosen cannot be done with high precision and would be but an approximation at the best. However, this approximation is not so bad because the extreme wavelengths in any one of the eight patterns differ from the central wavelength by only 2%. Now in a Fresnel single slit pattern the first minimum does not have zero intensity but the fact that the measured pattern does have a very low value is an indication that the minima of the eight patterns are falling closely together and hence any one pattern resembles closely the resultant pattern, which means that the correction of summing up several representative patterns institutes some degree of accuracy in the pattern. In fact, it can be seen from Table VI that the extreme patterns differ from the average pattern by less than 10% and therefore the average pattern should be correct well within this limit.

For the calculation of the width of the diffraction slit the determination of the average wavelength can be made with fair accuracy but the assumption that the minimum due to this average wavelength will fall at the same place as the average minimum must have some error. Because of the relative slopes on the two sides of the minimum, the minimum of the pattern of the average wavelength will probably lie slightly closer to the center of the pattern than the minimum of the average pattern. This can be qualitatively seen by inspection of Table VI. The width of the pattern is very sensitive to changes in the width of the slit. The pattern would be but

one half as wide, for instance, if in this particular case the width of the slit had been taken as the estimated value which was 25% greater than the calculated value which was used in the calculation of the theoretical pattern. In the calculated pattern of Fig. 18 a decrease in width of the pattern of about 5% would, taking into account the slight resultant increase in the value of the maximum, bring the calculated and theoretical patterns into coincidence, within the remaining limits of error of the two curves. This decrease of five percent in width of pattern would be brought about by an increase of about 2.5% in the slit width, but the slit width is only calculated to an accuracy of one part in 28 or 3.6% and the pattern as calculated is therefore in agreement with the measured pattern within the probable error of the calculations.

Errors due to reading the spiral range from 2 to 10 percent, depending upon the magnitude of the reading, the gross errors appearing in the small values where the greatest discrepancy exists between the calculated and theoretical values.

No correction was made for the width of the filament of the source. This width of 0.0025 cms. is but a fraction of the width of the slit in front of the cell. Where the width of the filament caused a slight diffuseness of the pattern the cell slit was wide enough to pick up the same light that it would have picked up had the filament been infinitely thin and this error is entirely negligible.

CONCLUSIONS

This experiment leads to the following conclusions:

1. For the thermionic amplification of very small photoelectric currents, where the dark current of the cell is comparable to the photoelectric current, good results are obtained by connecting the cell to the thermionic tube in the fashion of a grid leak whose resistance is a function of the quantity of incident light and the potential across its terminals. This type of connection has the advantages of being specially sensitive in the region of lowest illumination and at the same time covering a considerable range. The usual connection has a more or less constant sensitivity and a definite practical upper limit for a given set of components. The circuit used in this experiment amplified currents ranging from about 10^{-15} to 10^{-12} amperes.

2. From consideration of the probable errors, it appears that the measured pattern is superior to the calculated one. This would indicate that for optical phenomena of this type using heterochromatic light, the resultant energy distribution can be more easily measured than calculated to the same degree of accuracy.

3. Within the sum of the two errors the measured and calculated Fresnel single slit patterns are similar. Before stating that they are identical this experiment would have to be repeated using monochromatic light,

Acknowledgement

The writer wishes to express his sincere appreciation to Dr. C. Duane Hause who gave freely of his time and helpful advice, to Professor C. W. Chapman whose kindness made this research possible, and to Mr. George Chapman for skillful mechanical assistance. Most of the figures were drawn by Mr. G. R. Camertsfelder.

LITERATURE CITED

1. Meyer, C. F., The Diffraction of Light, X-Rays, And Material Particles, pp. 53-73, University of Chicago Press, Chicago, 1934.

2. Lyman, Theodore, The Distribution of Light Intensity In A Fresnel Diffraction Pattern From A Straight Edge, Proceedings of The National Academy of Sciences 16: 71-74, 1930.

3. DuBridge, L. A. and Brown, Hart, An Improved D.C. Amplifying Circuit, Review of Scientific Instruments 4: 532-536, 1933.

4. Soller, Walter, One-Tube Balanced Circuit For D.C. Vacuum Tube Amplifiers Of Very Small Currents, Review Of Scientific Instruments 3: 416-422, 1932.

5. MacDonald, P. A., The Thermionic Amplification Of Direct Currents, Physics 7: 295-296, 1936.

6. Sparrow, C. M., Table Of Fresnel Integrals, Edwards Brothers, Inc., Ann Arbor, Mich., 1934.

7. Forsythe, W. E. and Worthing, A. G., The Properties Of Tungsten And The Characteristics Of Tungsten Lamps, Abstract-Bulletin Of Lamp Development Laboratory Of General Electric Company 2: 6-12, 1930.

8. Russell, John, A Photoelectric Cell Circuit With A Logarithmic Response, Review Of Scientific Instruments 8: 495-496, 1937.